JOC Article

Structure−Property Investigations of Conjugated Thiophenes Fused onto a Dehydro[14]annulene Scaffold

Matthew J. O'Connor, Robert B. Yelle,† Lev N. Zakharov, and Michael M. Haley*

Department of Chemistry and Materials Science Institute, University of Oregon, Eugene, Oregon 97403, and Computational Science Institute, University of Oregon, 5294 University of Oregon, 1600 Millrace Drive, Suite 105, Eugene, Oregon 97403,

haley@uoregon.edu

Received January 28, 2008

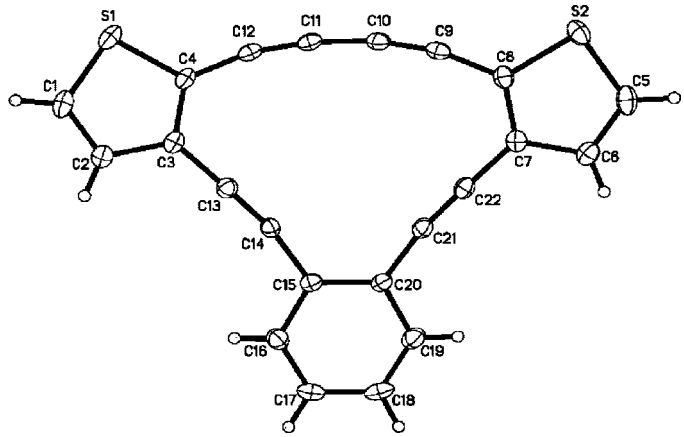

A series of 12 thieno-fused macrocycles based on the dehydro[14]annulene framework have been prepared. Studies have focused on the optical and electronic properties of the dehydrobenzothieno[14]annulenes (DBTAs) and dehydrothieno[14]annulenes (DTAs) utilizing NMR spectroscopy, UV−vis spectrophotometry, electrochemistry, and DFT computations. X-ray crystal structures were also obtained for two of the macrocycles. The structure−property relationships were found to vary significantly based on the relative orientation of the thiophenes. The stability, properties, and reactivity of these macrocycles were found to be more typical of dehydroannulenes rather than oligothiophenes.

Introduction

Highly unsaturated conjugated compounds have attracted considerable attention from both synthetic and theoretical chemists in recent years.[1] In particular, alkyne-containing systems[2] have garnered the bulk of this interest, which can be attributed to two main factors. First, the advent of new synthetic methodologies for the preparation of such molecules based on organometallic cross-coupling reactions[3] has provided access to a vast array of compounds whose preparation was not possible

* Corresponding author. Fax: 541-346-0487. Phone: 541-346-0456.
† Computational Science Institute, University of Oregon.

(1) Inter alia: (a) *Topics in Current Chemistry (Carbon Rich Compounds I)*; de Meijere, A., Ed.; Springer-Verlag: Berlin, Germany, 1998; Vol. *196*. (b) *Topics in Current Chemistry (Carbon Rich Compounds II)*; de Meijere, A., Ed.; Springer-Verlag: Berlin, Germany, 1999; Vol. 201. (c) Watson, M. D.; Fechtenkötter, A.; Müllen, K. *Chem. Rev.* **2001**, *101*, 1267–1300. (d) Grimsdale, A. C.; Müllen, K. *Angew. Chem. Int. Ed.* **2005**, *44*, 5592–5629. (e) *Carbon-Rich Compounds: From Molecules to Materials*; Haley, M. M., Tykwinski, R. R., Eds.; Wiley-VCH: Weinheim, Germany, 2006.

(2) Inter alia: (a) *Modern Acetylene Chemistry*, Stang, P. J., Diederich, F., Eds.; VCH: Weinheim, Germany, 1995. (b) Bunz, U. H. F.; Rubin, Y.; Tobe, Y. *Chem. Soc. Rev.* **1999**, *28*, 107–119. (c) Bunz, U. H. F. *Chem. Rev.* **2000**, *100*, 1605–1644. (d) Nielsen, M. B.; Diederich, F. In *Modern Arene Chemistry*; Astruc D., Ed.; Wiley-VCH: Weinheim, Germany, 2002; pp 196−216. (e) *Acetylene Chemistry: Chemistry, Biology, and Material Science*; Diederich, F., Stang, P. J., Tykwinski, R. R., Eds.; Wiley-VCH: Weinheim, Germany, 2005.

(3) (a) *Metal Catalyzed Cross-Coupling Reactions*, 2nd ed.; de Meijere, A., Diederich, F., Eds.; Wiley-VCH: Weinheim, Germany, 2004. (b) *Transition Metal Catalyzed Reactions—IUPAC Monographs Chemistry for 21st Century*; Davies, S. G., Murahashi, S., Eds.; Blackwell Science: Oxford, UK, 1998.

(4) (a) Spreiter, R.; Bosshard, C.; Knöpfle, G.; Günter, P.; Tykwinski, R. R.; Schreiber, M.; Diederich, F. *J. Phys. Chem. B* **1998**, *102*, 29–32. (b) Tykwinski, R. R.; Gubler, U.; Martin, R. E.; Diederich, F.; Bosshard, C.; Günter, P. *J. Phys. Chem. B* **1998**, *102*, 4451–4465. (c) Sarkar, A.; Pak, J. J.; Rayfield, G. W.; Haley, M. M. *J. Mater. Chem.* **2001**, *11*, 2943–2945. (d) Slepkov, A.; Hegmann, F. A.; Tykwinski, R. R.; Kamada, K.; Ohta, K.; Marsden, J. A.; Spitler, E. L.; Miller, J. J.; Haley, M. M. *Opt. Lett.* **2006**, *31*, 3315–3317. (e) Bhaskar, A.; Guda, R.; Haley, M. M.; Goodson, T., III *J. Am. Chem. Soc.* **2006**, *128*, 13972–13973.

10.1021/jo800225u CCC: $40.75
Published on Web 05/29/2008

before. Second, many of these carbon-rich molecules and macrocycles of higher dimensionality have been shown to exhibit interesting materials properties such as nonlinear optical (NLO) activity,[4] liquid crystalline behavior,[5] and molecular switching.[6] Furthermore, it has recently been demonstrated that dehydrobenzoannulenes[7] and related phenyl-acetylene macrocycles[8] are useful precursors to a number of carbon-rich polymeric systems, such as molecular tubes,[9] ladder polymers,[10] and novel allotropes of carbon.[11] It is therefore imperative to have ready access to a wide variety of these high carbon content molecules in sufficient quantities via easy synthetic processes if their technological potential is to be harnessed.

We have been investigating alkyne-rich dehydrobenzoannulenes (DBAs)[7,12] with the aim of exploring their diverse chemical and physical properties. Over the past decade, our group has developed new or improved existing synthetic techniques for the preparation of such macrocycles. As one particular consequence, it is now possible to introduce donor and/or acceptor functional groups on the phenyl rings of the DBA in a discrete manner, thus effectively "tuning" the electronic and optical properties of the annulene.[12a] In our continuing endeavor to introduce more variations in the DBA structure for detailed structure−property relationship studies, we elected to incorporate thiophene moieties onto the dehydroannulene skeleton.[13] The choice of thiophene as the fused aromatic ring was inspired by factors such as the chemical and electrochemical polymerizability of thiophene, the ability to form two-dimensional π-systems useful for electronics and photonics, the easier polarizability of thiophene, and the interaction among the individual macrocycles due to the lone pairs on the sulfur in each thiophene ring.[14] Compared to other heteroaromatic

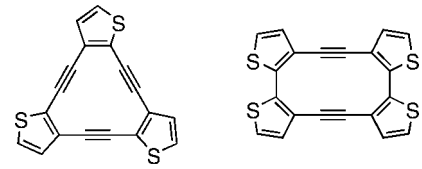

1 **2**

FIGURE 1. Examples of known dehydrothienoannulenes.

molecules, thiophenes are typically easier to handle and to functionalize than furans and pyrroles, allowing ready access to tailored thiophene derivatives. By locking the conjugated unit into planarity, thiophene-containing macrocycles[15] and cyclic thiophene−acetylene hybrids[16–18] have the potential to be more efficient materials due to enforced π-orbital overlap, increasing the quinoidal character of the delocalized system and thus lowering the HOMO−LUMO energy gap.[19]

Previous work on dehydrothienoannulenes (DTAs, Figure 1) by the groups of Youngs (e.g., **1**)[17] and Marsella (e.g., **2**)[18] relied on metal-mediated intermolecular couplings for molecule assembly. By virtue of the structure of the starting materials, only C_{nh}- and D_{nh}-symmetric macrocycles were produced. To probe the structure/property relationships among the various structural isomers, it is necessary to introduce the thiophene moieties in a systematic, stepwise manner to produce DTAs possessing lower symmetries (C_{2v}, C_s). Our initial communication focused on the [18]DTA skeleton;[13] however, stability problems with the thienyldiyne intermediates forced us to examine other topologies. This article describes the design and stepwise preparation of benzo/thieno-fused [14]DBTA hybrids **3**−**9** and the corresponding all-thiophene containing [14]DTAs **10**−**14** starting with a few common synthons (Figure 2). The solid state properties of **8** and **13** are investigated by X-ray crystallography. We also report the effect of structural variations on the overall effective conjugation of the macrocycles as determined by electronic absorption spectroscopy, electrochemistry, and DFT computations. Finally, we discuss the thermal properties of these macrocycles.

Results and Discussion

Macrocycle Synthesis. The use of building blocks **15**−**24** (Figure 3), which conforms to our previous strategies, is significant for streamlining synthetic efforts and making the

(5) (a) Zhang, J.; Moore, J. S. *J. Am. Chem. Soc.* **1994**, *116*, 2655–2656. (b) Pesak, D. J.; Moore, J. S. *Angew. Chem., Int. Ed. Engl.* **1997**, *36*, 1636–1639. (c) Seo, S. H.; Jones, T. V.; Seyler, H.; Peters, J. O.; Kim, T. H.; Chang, J. Y.; Tew, G. N. *J. Am. Chem. Soc.* **2006**, *128*, 9264–9265.

(6) (a) Gobbi, L.; Seiler, P.; Diederich, F. *Angew. Chem., Int. Ed.* **1999**, *38*, 674–678. (b) Gobbi, L.; Seiler, P.; Diederich, F.; Gramlich, V. *Helv. Chim. Acta* **2000**, *83*, 1711–1723.

(7) (a) Marsden, J. A.; Palmer, G. J.; Haley, M. M. *Eur. J. Org. Chem.* **2003**, 2355–2369. (b) Spitler, E. L.; Johnson, C. A.; Haley, M. M. *Chem. Rev.* **2006**, *106*, 5344–5386.

(8) (a) Jones, C. S.; O'Connor, M. J.; Haley, M. M., In ref 2e; pp 303−385. (b) Zhao, D.; Moore, J. S. *Chem. Commun.* **2003**, 807–818. (c) Zhang, W.; Moore, J. S. *Angew. Chem., Int. Ed.* **2006**, *45*, 4416–4439.

(9) Baldwin, J. P.; Matzger, A. J.; Scheiman, D. A.; Tessier, C. A.; Vollhardt, K. P. C.; Youngs, W. J. *Synlett* **1995**, 1215–1218.

(10) Zhou, Q.; Carroll, P. J.; Swager, T. M. *J. Org. Chem.* **1994**, *59*, 1294–1301.

(11) (a) Boese, R.; Matzger, A. J.; Vollhardt, K. P. C. *J. Am. Chem. Soc.* **1997**, *119*, 2052–2053. (b) Tobe, Y.; Nakagawa, N.; Naemura, K.; Wakabayashi, T.; Shida, T.; Achiba, Y. *J. Am. Chem. Soc.* **1998**, *120*, 4544–4545. (c) Rubin, Y.; Parker, T. C.; Pastor, S. J.; Jalisatgi, S.; Boulle, C.; Wilkins, C. L. *Angew. Chem., Int. Ed.* **1998**, *37*, 1226–1229. (d) Laskoski, M.; Steffen, W.; Morton, J. G. M.; Smith, M. D.; Bunz, U. H. F. *J. Am. Chem. Soc.* **2002**, *124*, 13814–13818.

(12) Recent contributions, inter alia: (a) Marsden, J. A.; Miller, J. J.; Shirtcliff, L. D.; Haley, M. M. *J. Am. Chem. Soc.* **2005**, *127*, 2464–2476. (b) Marsden, J. A.; Haley, M. M. *J. Org. Chem.* **2005**, *70*, 10213–10226. (c) Johnson, C. A.; Baker, B. A.; Berryman, O. B.; Zakharov, L. N.; O'Connor, M. J.; Haley, M. M. *J. Organomet. Chem.* **2006**, *691*, 413–421. (d) Anand, S.; Varnavski, O.; Marsden, J. A.; Haley, M. M.; Schlegel, H. B.; Goodson, T., III *J. Phys. Chem. A* **2006**, *110*, 1305–1318. (e) Spitler, E. L.; McClintock, S. P.; Haley, M. M. *J. Org. Chem.* **2007**, *72*, 6692–6699. (f) Johnson, C. A., II; Lu, Y.; Haley, M. M. *Org. Lett.* **2007**, *9*, 3725–3728. (g) Tahara, K.; Johnson, C. A., II; Fujita, T.; Sonoda, M.; De Schryver, F.; De Feyter, S.; Haley, M. M.; Tobe, Y. *Langmuir* **2007**, *23*, 10190–10197. (h) Spitler, E. L.; Monson, J. M.; Haley, M. M. *J. Org. Chem.* **2008**, *73*, 2211–2223. (i) Spitler, E. L.; Haley, M. M., *Org. Biomol. Chem.* **2008**, *6*, 1569–1576.

(13) (a) Sarkar, A.; Haley, M. M. *Chem. Commun.* **2000**, 1733–1734. (b) Sarkar, A.; Marsden, J. A.; Haley. M. M. Unpublished results.

(14) (a) Roncali, J. *Chem. Rev.* **1992**, *92*, 711–738. (b) Jen, A. K.; Rao, V. P.; Wong, K. Y.; Drost, K. J. *Chem. Commun.* **1993**, 90–91. (c) Zamboni, R.; Danieli, R.; Ruini, G.; Taliani, C. *Opt. Lett.* **1989**, *14*, 1321–1323.

(15) (a) Krömer, J.; Rios-Carreras, I.; Fuhrmann, G.; Musch, C.; Wunderlin, M.; Debärdemäker, T.; Mena-Osteritz, E.; Bäuerle, P. *Angew. Chem., Int. Ed.* **2000**, *39*, 3481–3486. (b) Bednarz, M.; Reineker, P.; Mena-Osteritz, E.; Bäuerle, P. *J. Lumin.* **2004**, *110*, 225–231. (c) Kozaki, M.; Parakka, J. P.; Cava, M. P. *J. Org. Chem.* **1996**, *61*, 3657–3661. (d) Hu, Z.; Scordilis-Kelley, C.; Cava, M. P. *Tetrahedron Lett.* **1993**, *34*, 1879–1882.

(16) (a) Mayor, M.; Didschies, C. *Angew. Chem., Int. Ed.* **2003**, *42*, 3176–3179. (b) Nakao, K.; Nishimura, M.; Tamachi, T.; Kuwatani, Y.; Miyasaka, H.; Nishinaga, T.; Iyoda, M. *J. Am. Chem. Soc.* **2006**, *128*, 16740–16747. (c) Bäuerle, P.; Cremer, J. *Chem. Mater.* **2008**, *20*, 2696–2703.

(17) (a) Solooki, D.; Bradshaw, J. D.; Tessier, C. A.; Youngs, R. J. *Organometallics* **1994**, *13*, 451–455. (b) Zhang, D.; Tessier, C. A.; Youngs, W. J. *Chem. Mater.* **1999**, *11*, 3050–3057. (c) See also: Iyoda, M.; Vorasingha, A.; Kuwatani, Y.; Yoshida, M. *Tetrahedron Lett.* **1998**, *39*, 4701–4704.

(18) (a) Marsella, M. J.; Kim, I. T.; Tham, F. *J. Am. Chem. Soc.* **2000**, *122*, 974–975. (b) Marsella, M. J.; Wang, Z.-Q.; Reid, R. J.; Yoon, K. *Org. Lett.* **2001**, *3*, 885–887. (c) Marsella, M. J.; Piao, G.; Tham, F. S. *Synthesis* **2002**, 1133–1135. (d) Marsella, M. J.; Reid, R. J.; Estassi, S.; Wang, L.-S. *J. Am. Chem. Soc.* **2002**, *124*, 12507–12510.

(19) (a) Takahashi, T.; Matsuoka, K.; Takimiya, K.; Otsubo, T.; Aso, Y. *J. Am. Chem. Soc.* **2005**, *127*, 8928–8929. (b) Kozaki, M.; Isoyama, A.; Okada, K. *Org. Lett.* **2005**, *7*, 115–118.

(20) (a) Gronowitz, S.; Vilks, V. *Ark. Kemi* **1964**, *21*, 191–196. (b) Gronowitz, S.; Holm, B. *Acta Chem. Scand. B* **1976**, *30*, 423–429. (c) Consiglio, G.; Gronowitz, S.; Hörnfeldt, A.-B.; Noto, R.; Spinelli, D. *Chem. Scr.* **1980**, *16*, 117–121. (d) Spagnoto, P.; Zaniroto, P.; Gronowitz, S. *J. Org. Chem.* **1982**, *47*, 3177–3180.

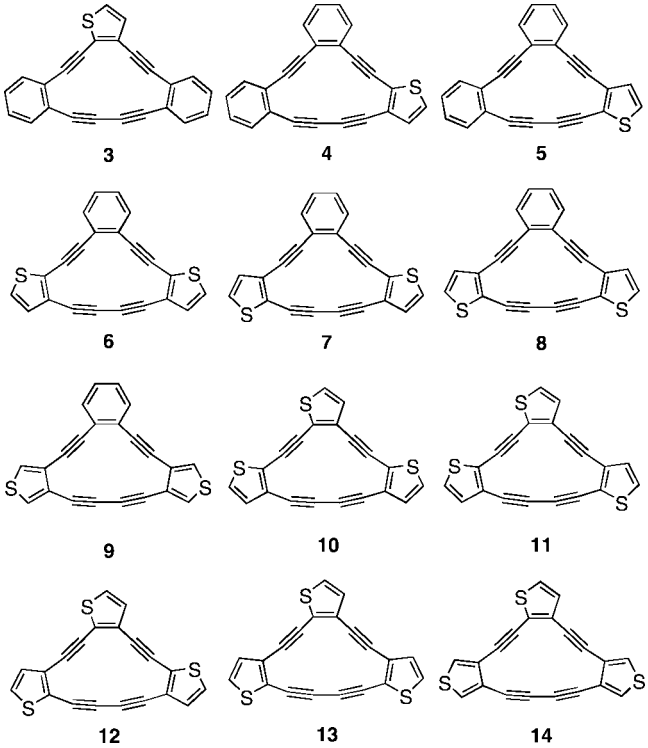

FIGURE 2. Target thieno-fused dehydro[14]annulenes **3**−**14**.

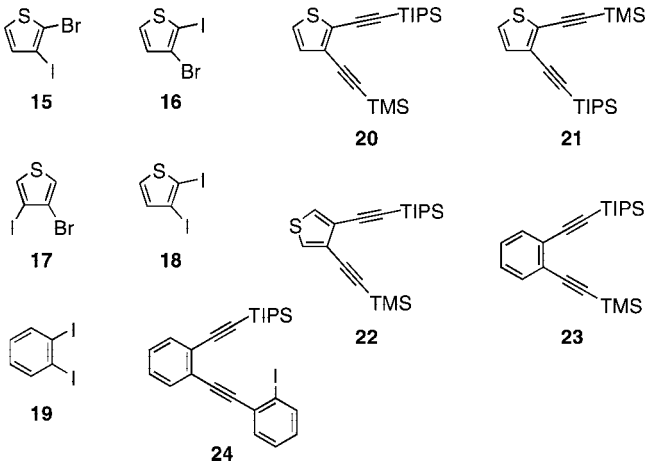

FIGURE 3. Building blocks **15**−**24**.

TABLE 1. Yields for Preparation of Differentially Protected Diynes 20−22

dihalothiophene	yield of TMSA cross-coupling	yield of TIPSA cross-coupling (pdt)
15	96%	95%, **20**
16	94%	92%, **21**
17	95%	93%, **22**

assembly of thiophene-based dehydro[14]annulenes relatively convenient and facile. All macrocycles reported herein were constructed starting from the appropriate dihalothiophenes **15**−**18**, which were in turn prepared from commercially available thiophenes following known procedures.[20] Halides **15**−**17** were subsequently converted into differentially protected diynes **20**−**22** by sequential Sonogashira cross-coupling with (trimethylsilyl)acetylene (TMSA) and (triisopropylsilyl)acetylene (TIPSA) in excellent yields (Table 1). The remaining pieces

SCHEME 1. Synthesis of "Symmetrical" [14]DBTA 6

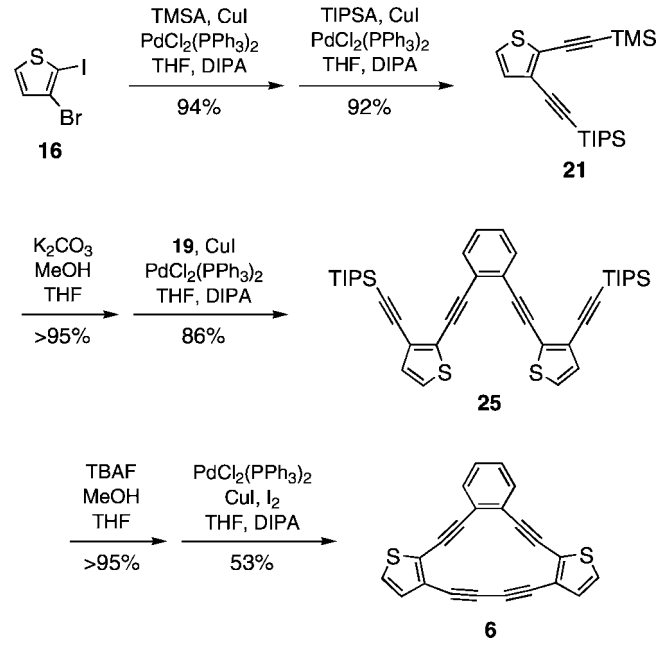

were either commercially available (**19**) or prepared by literature methods (**23**, **24**).[21]

[14]DBTAs **3**, **6**, **8**, and **9** and [14]DTAs **10**, **13**, and **14** possess two fused benzenes or two fused thiophenes in a symmetrical orientation on the lower portion of the annulene, and thus were assembled by using a 2-fold coupling of the respective diyne to a central dihaloarene core. Scheme 1 illustrates a representative synthesis starting from **16**. Sequential Sonogashira reactions with TMSA and TIPSA (the latter requiring elevated heating over several days for completion) afforded diyne **21** in 91% yield for the two steps. Selective removal of the TMS group with K_2CO_3 in MeOH followed by cross-coupling to 1,2-diiodobenzene (**19**) furnished tetrayne **25** in 86% yield. Protiodesilylation with TBAF and subsequent acetylenic homocoupling utilizing $PdCl_2(PPh_3)_2$ catalyst, CuI cocatalyst, and iodine as an oxidant[22] gave hybrid **6** in 53% yield.

[14]DBTAs **4**, **5**, and **7** and [14]DTAs **11** and **12** possess two different fused arenes or two fused thiophenes in unsymmetrical orientations on the lower portion of the annulene, and are thus formed by sequential cross-couplings to the dihaloarene "crown". [14]DBTAs **4** and **5** were prepared by cross-coupling **21** and **22** to previously reported halodiyne **24**.[21] Scheme 2 shows a representative synthesis of an "unsymmetrical" macrocycle, DTA **12**. Starting diyne **21** was desilylated with mild base and then immediately cross-coupled to **15**. The resulting halodiyne was cross-coupled to monodesilylated **20** to give **26** in a combined 80% yield. The macrocyclization step was performed as before utilizing the Pd(II)/Cu(I) catalyst system under oxidizing conditions, affording **12** in 64% yield. Use of more traditional $CuCl/Cu(OAc)_2$ in pyridine for the homocoupling reactions[22b] afforded the DTAs in comparable yields. A summary of the syntheses off all 12 macrocycles is given in Table 2.

(21) (a) Haley, M. M.; Bell, M. L.; English, J. J.; Johnson, C. A.; Weakley, T. J. R. *J. Am. Chem. Soc.* **1997**, *119*, 2956–2957. (b) Bell, M. L.; Chiechi, R. C.; Johnson, C. A.; Kimball, D. A.; Matzger, A. J.; Wan, W. B.; Weakley, T. J. R.; Haley, M. M. *Tetrahedron* **2001**, *57*, 3507–3520.

(22) (a) Marsden, J. A.; Miller, J. J.; Haley, M. M. *Angew. Chem., Int. Ed.* **2004**, *43*, 1694–1697. (b) See also: Siemsen, P.; Livingston, R. C.; Diederich, F. *Angew. Chem., Int. Ed.* **2000**, *39*, 2632–2657.

SCHEME 2. Synthesis of "Unsymmetrical" [14]DTA 12

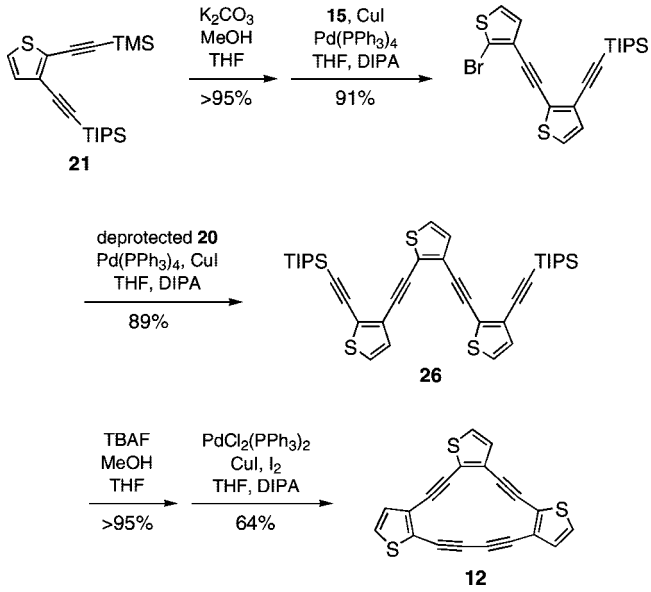

Unlike related DBA structures, the thieno-fused annulenes exhibit moderate to poor stability during workup and are sensitive to acid, light, and silica, which accounts for the lower than normal cyclization yields. Workups were more successful when avoiding halogenated solvents and utilizing fast chromatographic methods (chromatotron or flash chromatography). NMR characterization of the annulenes was done primarily in deuterated benzene, dichloromethane, or tetrahydrofuran. In general, those molecules with UV−vis absorptions greater than 400 nm showed the most sensitivity and/or where both sulfurs are oriented "down" (sulfur α to the diacetylene linkage) as is the case with **8** and **13**. Most macrocycles could be stored in solution or in the solid state for a few days if kept cold and dark under argon.

DSC analyses of **3**−**14** show that the macrocycles polymerize/decompose prior to melting to afford black solids. Hybrids **3**−**8** exhibit somewhat sharp exotherms, with **6** where the sulfurs are oriented "up" reacting at a higher temperature (190 °C) than isomer **8** where the sulfurs are oriented "down" (120 °C). In the case of the [14]DTAs **10**−**14**, the thermograms show two broad transitions occurring near 150 °C. All of the data are indicative of fairly disordered polymerizations. Complete decomposition of **3**−**14** proceeds rapidly after 200 °C.

X-Ray Structural Data. Single crystals of **8** and **13** suitable for X-ray diffraction were obtained by slow vapor diffusion of pentane into THF solutions of the macrocycle. The X-ray structure and the crystal packing of hybrid **8** are shown in Figure 4. The main structural unit of **8** consists of layers of four molecules joined by intermolecular $\pi\cdots\pi$ and S···S interactions. Two molecules lie in the same plane (coplanar within 0.12 Å) and are additionally connected by two S···S interactions (S···S distances of 3.61 Å). The remaining two molecules are above and below the average plane of the pair in such a fashion that the four S atoms in these molecules form a rectangle with S···S distances in the range 3.75−3.88 Å. In the crystal these structural units are connected by much weaker S···S contacts (4.10 Å), forming infinite chains. The arrangement of the molecules clearly indicates that intermolecular S···S interactions play an important role in the association of the molecules in the crystal structure of **8**, and are in good agreement with known directional preferences of nonbonded atomic S···S contacts with divalent sulfur, which could be explained based on its orbital orientation.[23]

The packing of the molecules in the crystal structure of [14]DTA **13** is different than that found in **8**. The two nearest molecules have opposite orientation to form pairs (Figure 5a) and these pairs are stacked in the crystals of **13** in columns (Figure 5b). Most of the S···S intermolecular contacts are in the range 3.60−3.82 Å and thus are comparable with typical intermolecular S···S contacts.[23] The four-molecule packing arrangement found in **8** is not present in **13**. The S(3) atoms in both symmetrically independent molecules are disordered over two positions, which indicates that there are no directional preferences of nonbonded atomic S···S contacts in **13**. Interestingly, neither crystal structure contains the packing motif conducive for topochemical polymerization,[24] which is found in the parent [14]DBA **27**,[25] nor are the α-positions of the thiophenes in reasonable proximity for subsequent reactivity. This likely explains the broad featureless exotherms observed in the DSC scans.

The molecular structures of **8** and **13** are essentially planar and show the typical bowed diacetylenic linkage of the strained dehydro[14]annulene core.[25,26] The sp-carbon bond angles of the diyne bridges in **8** (166.3(3)−169.0(3)°) and **13** (166.9(4)−170.9(4)°) are nearly the same as those in **27** (168.8−171.4°). For the monoyne linkages less strain is contained in the sp-carbon nearer the diyne unit (175.2(3)−178.9(3)°) than the sp-carbon proximal to the arene "crown" (168.5(3)−174.2(3)°).

NMR Analysis. Previous work on the octadehydro[14]annulene framework, common to molecules **3**−**14** as well, examined the effects of thienoannelation and successive benzannelation (e.g., **27**−**29**, Figure 6) upon the diatropicity of the 14-membered ring.[27] Experimentally these alterations were studied by analyzing the changes of the NMR chemical shifts of the alkene protons within the series of macrocycles and with their acyclic precursors. Such effects can also be observed on the fused-benzene and thiophene protons due to ring-current competition, though to a smaller degree.[28] Although they do not possess sensitive alkene protons, annulenes **3**−**14** exhibit distinct downfield shifts of their arene protons upon cyclization, indicative of a diatropic current in the central 14-membered core. As opposed to an exhaustive discussion of all 12 annulenes, we will focus on [14]DBTAs **6**−**9** due to the two different aryl groups and C_{2v}-symmetry (or near symmetry), which makes interpretation of the data easier. The arene proton chemical shifts of **6**−**9** and of their acyclic precursors along with the corresponding data for **27**−**29** are given in Table 3.[29] The proton labeling scheme is shown in Figure 6.

Examination of the ^{1}H NMR spectra of all seven precyclized molecules shows that the range of chemical shifts of the distal and proximal benzene protons (A and B, respectively) is

(23) Guru Row, T. N.; Parthasarathy, R. *J. Am. Chem. Soc.* **1981**, *103*, 477–479.
(24) Enkelmann, V. *Adv. Polym. Sci.* **1984**, *63*, 91–136.
(25) Baldwin, K. P.; Matzger, A. J.; Scheiman, D. A.; Tessier, C. A.; Vollhardt, K. P. C.; Youngs, W. J. *Synlett* **1995**, 1215–1218.
(26) Blanchette, H. S.; Brand, S. C.; Naruse, H.; Weakley, T. J. R.; Haley, M. M. *Tetrahedron* **2000**, *56*, 9581–9588.
(27) (a) Boydston, A. J.; Haley, M. M. *Org. Lett.* **2001**, *3*, 3599–3601. (b) Boydston, A. J.; Haley, M. M.; Williams, R. V.; Armantrout, J. R. *J. Org. Chem.* **2002**, *67*, 8812–8819.
(28) (a) Matzger, A. J.; Vollhardt, K. P. C. *Tetrahedron Lett.* **1998**, *39*, 6791–6794. (b) Wan, W. B.; Kimball, D. B.; Haley, M. M. *Tetrahedron Lett.* **1998**, *39*, 6795–6798.
(29) Baldwin, K. P.; Bradshaw, J. D.; Tessier, C. A.; Youngs, W. J. *Synlett* **1993**, 853–855.

TABLE 2. Synthesis and Yields of DBTAs and DTAs 3−14

	"equivalents" of monodesilylated diyne					
haloarene	**20**	**21**	**22**	**23**	precursor, yield	annulene, yield
18				2	pre-**3**, 90%	**3**, 62%
24		1			pre-**4**, 89%	**4**, 29%
24	1				pre-**5**, 64%	**5**, 33%
19		2			pre-**6** (**25**), 86%	**6**, 53%
19	1 (second)	1 (first)			pre-**7**, 15%	**7**, 33%
19	2				pre-**8**, 90%	**8**, 32%
19			2		pre-**9**, 61%	**9**, 37%
18		2			pre-**10**, 67%	**10**, 30%
15	1 (first)	1 (second)			pre-**11**, 28%	**11**, 30%
15	1 (second)	1 (first)			pre-**12** (**26**), 81%	**12**, 64%
18	2				pre-**13**, 52%	**13**, 45%
18			2		pre-**14**, 47%	**14**, 38%

extremely small: 7.30−7.36 ppm for A and 7.50−7.56 ppm for B. These values are essentially the same as in 1,2-diethynylbenzene (7.29 and 7.50 ppm),[28b] suggesting very little or no influence from the group(s) appended at the end of the 1,2-diethynyl linkages. Upon macrocyclization, protons A and B in **6**−**8** move downfield to 7.58−7.61 and 8.09−8.12 ppm, respectively. Although **6**−**8** differ in the orientation of the thiophene rings, the results show that this structural variation has no effect on the remotely located benzene protons. The changes in shifts, $\Delta\delta \approx 0.25$ ppm for A and 0.55 ppm for B, are similar in magnitude to those in **28**, which suggests that two 2,3-fused thiophene rings have approximately the same bond-fixing ability as one fused benzene ring.[30]

Interestingly, 3,4-fusion of the two thiophenes in **9** results in downfield shifts of protons A and B about half as large as those in **6**−**8**, and slightly smaller than in **27**. The 3,4-bond in a

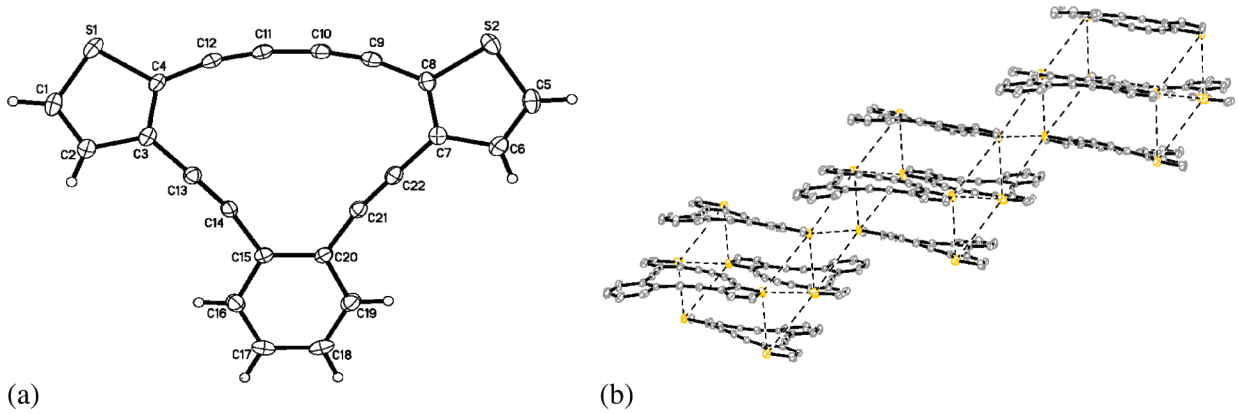

FIGURE 4. (a) X-ray structure of [14]DBTA **8**; ellipsoids at the 30% probability level. (b) Fragment of the crystal packing of **8** showing S···S interactions.

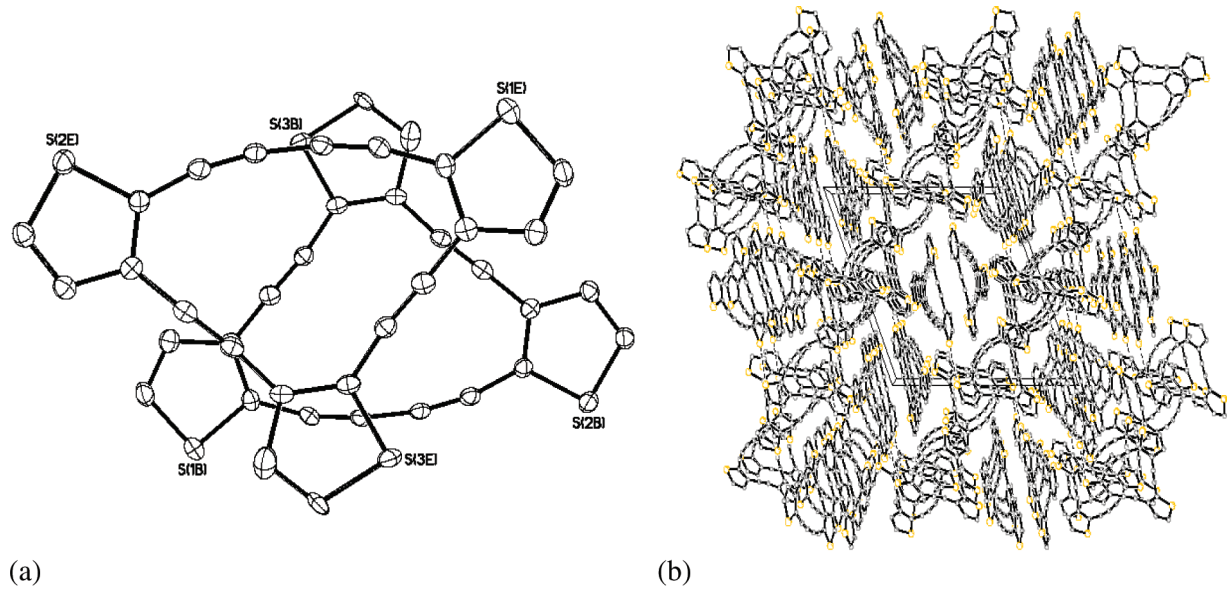

FIGURE 5. (a) X-ray structure of [14]DTA **13**; ellipsoids drawn at the 30% probability level. Only one position for the disordered atoms is shown. (b) Crystal packing of **13**.

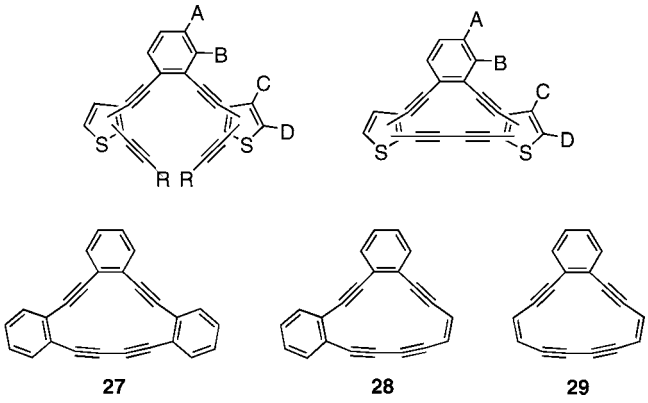

FIGURE 6. Proton labeling scheme in Table 3 for hybrids **6**−**9** and known [14]annulenes **27**−**29**.

TABLE 3. ^{1}H NMR Chemical Shifts (δ, ppm) of [14]DBTAs 6−9 and Their Precursor Tetraynes in CD_2Cl_2, and Comparison with Known [14]DBAs 28−30

	benzene		thiophene	
compd	proton A	proton B	proton C	proton D
25 (pre-**6**)	7.36	7.55	7.24	7.07
6	7.61	8.10	7.53	7.26
pre-**7**	7.34	7.53, 7.51	7.22, 7.15	7.13, 7.07
7	7.61, 7.58	8.12, 8.09	7.60, 7.53	7.50, 7.25
pre-**8**	7.33	7.52	7.19	7.04
8	7.60	8.12	7.60	7.51
pre-**9**	7.30	7.52	7.49	7.45
9	7.39	7.75	7.75	7.47
pre-**27**[a]	7.34	7.56		
27[b]	7.43	7.89		
pre-**28**[c]	7.33	7.54		
28[c]	7.64, 7.56	8.11, 7.99		
pre-**29**[c]	7.32	7.50		
29[c]	7.72	8.28		

[a] Reference 29; in C_6D_6. [b] Reference 25; in $CDCl_3$. [c] Reference 27b.

thiophene ring is well-known to possess less double bond character than the 2,3-bond.[31] This results in less efficient delocalization in the 14-membered nucleus of **9** and thus poorer bond-fixing ability compared to that of **6**−**8**. Alternatively, the difference in character between **6**−**8** and **9** can also be explained by viewing **9** as a dehydrobisthia[20]annulene with two zero-bridges, in which 22 π-electrons are delocalized over the whole periphery, while **6**−**8** are bisthieno-annelated dehydro[14]annulenes. Following the usual trend, the larger annulene **9** is less aromatic than the effectively smaller annulenes **6**−**8**.[7b]

Thiophene protons C and D resonate in the range of 7.04−7.13 and 7.15−7.24 ppm for the precyclized molecules, and move ca. 0.3−0.4 ppm downfield upon forming **6**−**8**. In general the thiophene doublets are farther downfield when the thiophenes are oriented "down" (e.g., **8**) compared to the isomers with the thiophenes oriented "up" (e.g., **6**). As with the benzene proton shifts above, asymmetric **7** displays features that are a combination of both **6** and **8** (Table 3). In the case of **9**, the thiophene proton shifts and change in shifts are comparable to those for **6**−**8**. While puzzling, we will table further discussion to avoid the possibility of overinterpretation.

Electronic Absorption Spectra. The electronic absorption spectrum of parent [14]DBA **27** shows a weak, low-energy absorption at 365 nm.[25] In comparison, the analogous band in the spectra of monothiophenes [14]DBTAs **3**−**5** (Figure 7a) displays a gradual bathochromic shift indicative of a narrowing of the HOMO−LUMO energy gap. Replacing the benzene "crown" with a 2,3-fused thiophene as in hybrid **3** shifts this absorption to 378 nm. Macrocycles **4** and **5**, where a 2,3-fused thiophene has replaced one of the side benzene rings, afford absorption bands at 386 and 391 nm, respectively. Incorporating a thiophene into the macrocycle slightly increases the dipole moment, while thiophene orientation affects the net dipole moment as the sulfur orientation changes from "up" in **4** to "down" in **5**.

The UV−vis spectra of the macrocycles incorporating two thiophenes are given in Figure 7b. As noted above, changing the sulfur atom orientation from "up" to "down" progressively shifts the low-energy absorption further into the red, from 373 nm for **6** (both "up") to 398 nm for **7** ("alternating"), then to 408 nm for **8** (both "down"). The extinction coefficients for similar bands also increase correspondingly. In the case of [14]DTA **9**, however, this band blue shifts to 339 nm, reflecting the weaker conjugation of the 3,4-fusion of both thiophenes and analogous to behavior previously observed for the larger [18]DTAs.[13]

Interestingly, the absorption spectra show little difference between **6**−**8** and **10**−**13**, where in the latter series three thiophenes are 2,3-fused onto the dehydro[14]annulene backbone (Figure 7c). The most red-shifted is DTA **13** at 408 nm (sulfurs "down"), the same wavelength as **8**, while the most blue-shifted annulene is **12** at 395 nm (sulfurs "alternating"). DTAs **10** and **11** share approximately the same peak at 400 nm and have very similar UV−vis absorption spectra. As before, switching to 3,4-fusion as in **14** results in weaker overall conjugation and thus the lowest energy band appears at 368 nm. Changing solvents from CH_2Cl_2 to toluene results in nearly identical absorption spectra for **3**−**14**. The observed electronic transitions for this class of macrocycles are most likely $\pi \rightarrow \pi^*$ with small variations in vibronic structure.

Electrochemistry. Cyclic voltammograms (CV) were taken of macrocycles **6**−**14** with use of a Pt disk working electrode, Ag wire reference, and Pt swirl auxiliary in CH_2Cl_2 solutions of TBAHFP and referenced to ferrocene. Table 4 lists the energies for the first oxidation and first reduction waves for **6**−**14**; representative CVs are given in the Supporting Information. Unlike a majority of thiophenes, which produce well-behaved CVs, the CVs of the DBTAs and DTAs were complex. Scanning in the positive potential direction generated one and sometimes two irreversible oxidations, while scanning negatively produced three (sometimes more) quasireversible reductions. The oxidation peak became more difficult to find when the oxidation peak occurred either at or concurrently with the CH_2Cl_2 solvent window. Unlike previous studies of thiophene−acetylene hybrids,[16,17] inclusion as part of the dehydro[14]annulene framework clearly alters the typical redox behavior of a thiophene moiety in a deleterious manner.

Computations. DFT calculations (B3LYP/6-311G**)[32] were performed on [14]DBTAs **6**−**9** and [14]DTAs **10**−**14** to help elucidate the observed trends. The calculated HOMO−LUMO energy gaps from the optimized structures, along with the HOMO−LUMO gaps experimentally determined from optical and electrochemical data, are given in Table 4. Although the computed values overestimate the experimental HOMO−LUMO

(30) Mitchell, R. H. *Chem. Rev.* **2001**, *101*, 1301–1316.
(31) Fringuelli, F.; Marino, G.; Taticchi, A. *J. Chem. Soc., Perkin Trans.* **1974**, *2*, 332–337.
(32) (a) Becke, A. D. *Phys. Rev. A* **1988**, *38*, 3098–3100. (b) Lee, C.; Yang, W.; Parr, R. G. *Phys. Rev. B* **1988**, *37*, 785–789. (c) Becke, A. D. *J. Chem. Phys.* **1993**, *98*, 5648–5652. (d) Becke, A. D. *J. Chem. Phys.* **1993**, *98*, 1372–1377.

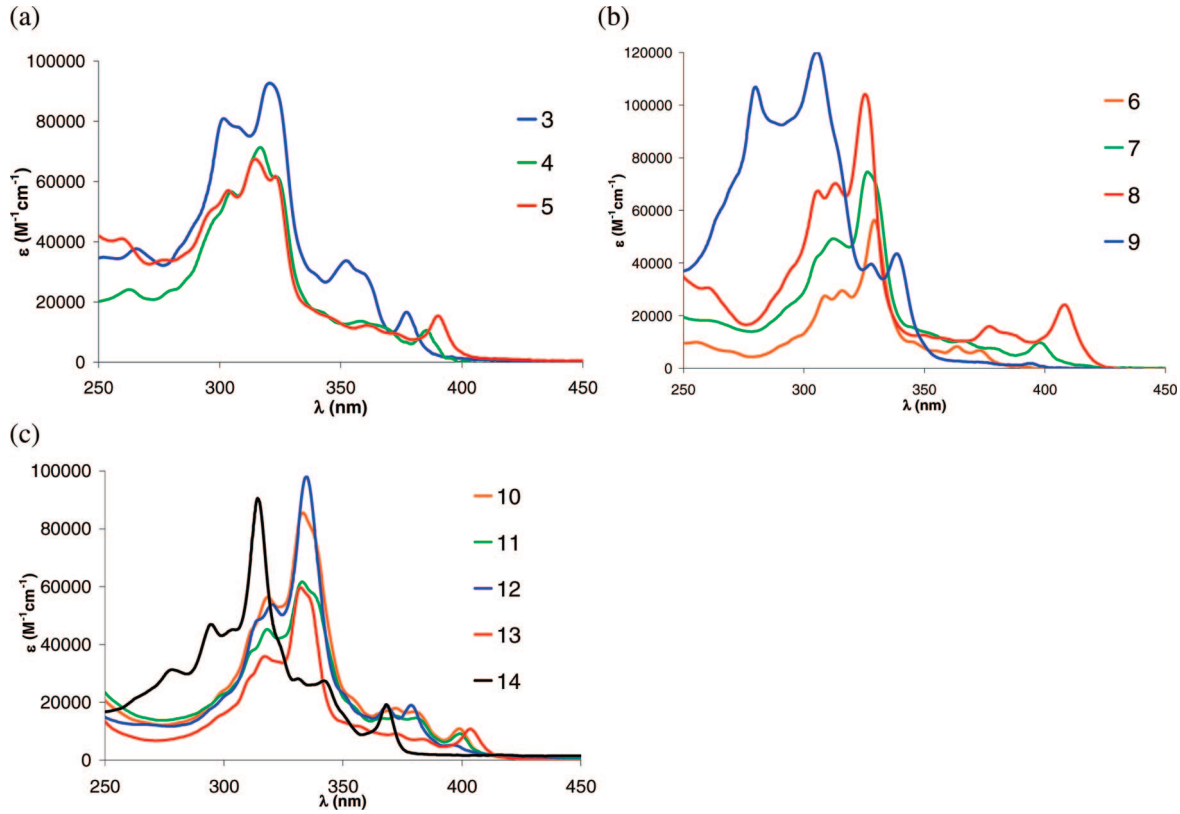

FIGURE 7. UV−vis absorption spectra of (a) **3**−**5**, (b) **6**−**9**, and (c) **10**−**14**. All spectra recorded in CH_2Cl_2 at analyte concentrations of 15−25 μM.

TABLE 4. HOMO-LUMO Energy Level Correlations of Selected [14]DBTAs and [14]DTAs

compd	lowest energy abs. λ_{max} [nm] (cutoff)	optical energy gap [eV]	electrochemical energy gap [eV]	DFT calcd energy gap [eV]	Epa (ox) (vs Fc) (calcd Epa)[a] [V]	Epc (red) (vs Fc) [V]	calcd Dipole [D]
6	374 (380)	3.26	3.26	3.53	1.39 (1.10)	−1.87	1.46
7	398 (410)	3.12	3.12	3.39	1.38 (1.04)	−1.74	2.91
8	408 (420)	3.04	2.93	3.26	1.12 (0.97)	−1.81	3.99
9	339 (360)	3.66	3.39	3.97	1.60 (1.24)	−1.79	2.33
10	399 (410)	3.10	2.87	3.37	1.13 (1.01)	−1.74	1.02
11	399 (410)	3.10	2.72	3.41	1.19 (0.97)	−1.54	2.58
12	395 sh (410)	3.16	3.09	3.48	1.32 (1.06)	−1.77	2.08
13	404 (414)	3.06	2.82	3.34	1.18 (1.05)	−1.64	3.53
14	368 (370)	3.37	3.39	3.63	1.62 (1.13)	−1.81	1.66

[a] The second number is the DFT calculated Epa value [V].

gaps, the numbers are in good overall agreement with the observed trends. For hybrids **6**−**9**, the ordering of the energy gaps is in excellent agreement among all three methods. The narrowest energy gap (2.93−3.26 eV) corresponds to **8** with the sulfurs "down", while the widest energy gap (3.39−3.97 eV) corresponds to **9**, attributable to the 3,4-fusion of the thiophenes. Macrocycles **6** (sulfurs "up") and **7** (sulfurs "alternating") lie in between these bookend values (Table 4).

For all-thiophene DTAs **10**−**14**, there is excellent agreement of energy gap ordering between the calculated and optically determined numbers. Given the aforementioned difficulties in obtaining the CVs, it is not surprising that ordering in the electrochemical data is slightly off for the 2,3-fused systems. Nonetheless, 3,4-fused DTA **14** has the widest energy gap (3.37−3.63 eV) analogous to **9**. As with **8**, the sulfurs "down" orientation of **13** is the smallest value of the all-thiophene series, in excellent agreement with the optical energy gap trend, and in close agreement with the electrochemical energy gap trend.

The pattern of relative sulfur orientation ("up", "down", "alternating") and the resulting effect on optoelectronic properties, while not observed for the [18]DTAs,[13] is an unmistakable feature in the [14] series. One possible correlation is the increase in dipole moment (Table 4): as the sulfur orientation switches from "up" to "alternating" then to "down", there is a small increase in the dipole moments and thus diminishing energy gaps. The dipole moments, however, are sufficiently small to begin with, which accounts for the apparent lack of solvatochromism. Another consideration is the repulsion between the sulfur electrons adjacent to the bowed alkynes. When examining thiophene cyclooligomers, the sulfur−sulfur repulsion of a bent chain, as in the case of Bäuerle's cyclic thiophenes,[15] blue-shifts the absorption spectra of the molecule with respect to a linear oligomer containing the same number of repeat units. A similar interaction could be operational between the sulfur lone pair of an "up" thiophene and the alkyne π-orbital of the bowed monoyne, thus causing the hypsochromic shifts. An alternative

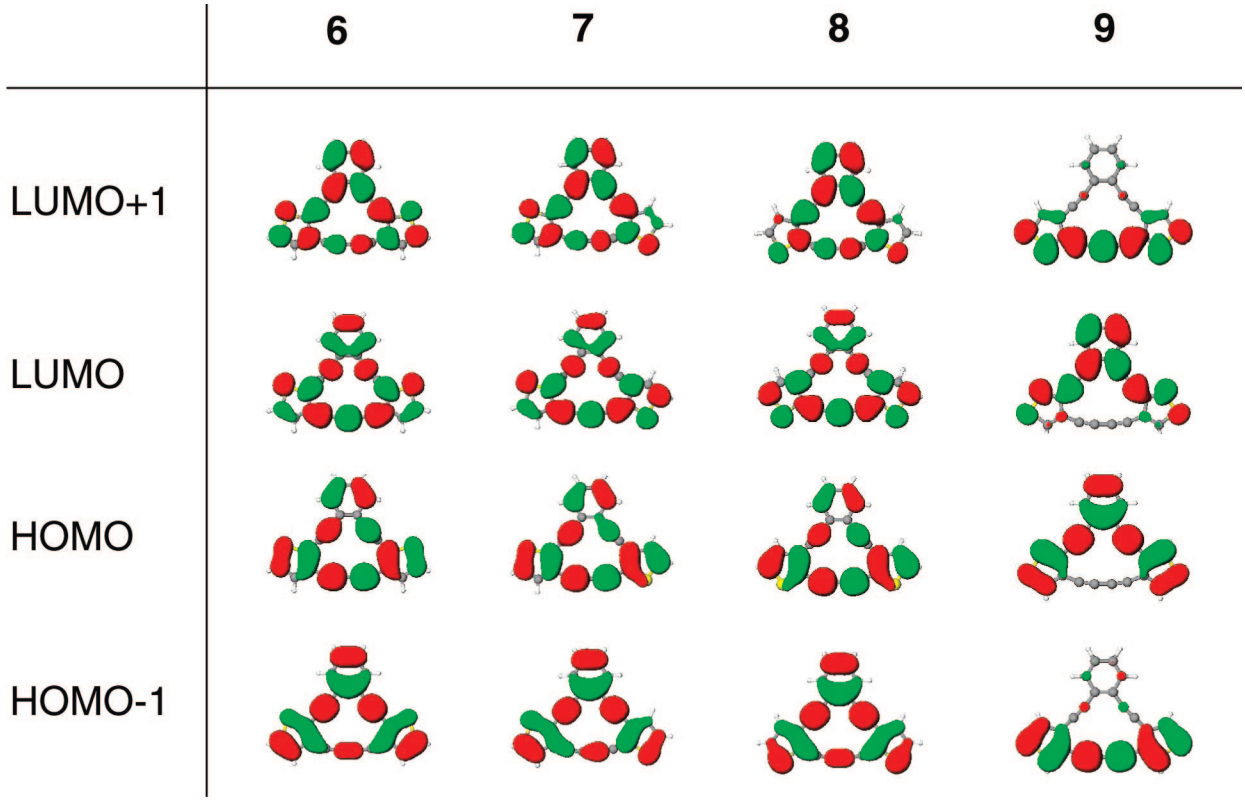

FIGURE 8. Calculated HOMO/LUMO plots of [14]DBTAs **6**−**9**.

view would be a decreased interaction between the sulfur lone pair of a "down" thiophene and the alkyne π-orbital of the bowed diyne linkage, resulting in bathochromic shifts. We are pursuing further experimental and computation studies to ascertain the exact cause of this effect.

The computed molecular orbital plots for **6**−**14** (Figure 8 for **6**−**9**, Figure S1 in the Supporting Information for **10**−**14**) show that there is little charge separation in the HOMOs and LUMOs across the entire series of molecules, thus confirming the $\pi \rightarrow \pi^*$ nature of the transitions in the electronic absorption spectra. For example, macrocycles **6**−**8** have HOMOs and LUMOs that topologically look very similar; thus, it is difficult to glean any meaningful information regarding the effects of sulfur orientation. The same can be said for DTAs **10**−**13**. The orbital plots for **9** and **14**, however, illustrate the dramatic difference between 2,3-fused and 3,4-fused macrocycles. The order of the HOMOs and LUMOs is swapped, i.e., the HOMO and LUMO of **6**−**8** and **10**−**13** correspond to the HOMO−1 and LUMO+1, respectively, of macrocycles **9** and **14**. In addition, HOMO−LUMO electron density of **9**/**14** is concentrated on the 1,2-bis(thienylethynyl)benzene portion of the molecule, not the diacetylene linkage. The electron density shifts to the diacetylene in the HOMO−1 and LUMO+1. The 3,4-fusion, and thus reduced double bond character, significantly disrupts the net conjugation of the entire macrocycle.

Conclusions

A series of 12 dehydro[14]annulene macrocycles successively fused with one (**3**−**5**), two (**6**−**9**), or three thiophene rings (**10**−**14**) have been prepared. Locking the entire π-system into planarity helps to promote orbital overlap, optical tunability, and increased ring currents in the macrocycles. The net electronic delocalization of these annulenes is greater than that of previously reported thiophene macrocycles, attributable to the rigid structure and aromatic nature of the [14]DBA ring further enhanced by the electron richness of the thiophenes themselves. The downfield chemical shifts in the ^{1}H NMR spectra show evidence of increased delocalization and enhanced ring current. Furthermore, the arrangement and number of thiophenes in the macrocycle dramatically affects the HOMO−LUMO energy gaps of the molecules, with the "down" orientation of the sulfurs in 2,3-fused systems (**8**, **13**) affording the lowest energies, as confirmed by UV−vis, electrochemical, and computational data. These data also show that the 3,4-fused macrocycles (**9**, **14**) possess the highest HOMO−LUMO energy gaps. X-ray crystal structures of **8** and **13** exhibit solid-state packing behavior unfavorable toward topochemical polymerization, thus explaining the broad exotherms found from DSC scans. The electronic delocalization in the macrocycles most likely creates molecules more similar to dehydroannulenes than thiophene oligomers, accounting for the limited stability of the compounds and poorly behaved electrochemical studies. Future studies are focusing on alkyl-stabilized [14]DTAs and on closely related [15]DTAs; this work will be reported in due course.

Experimental Section

General Methods. These are described in ref 12a. Dihalothiophenes **15**−**17**[20] and diynes **21**,[12c] **23**,[21] and **24**[21] were prepared according to known procedures.

2-(Triisopropylsilylethynyl)-3-(trimethylsilylethynyl)thiophene (20). 2-Bromo-3-iodothiophene (**15**, 3.0 g, 10 mmol), CuI (125 mg, 0.7 mmol), and $PdCl_2(PPh_3)_2$ (251 mg, 0.033 mmol) were dissolved in DIPA (100 mL) and THF (100 mL). The solution was degassed under Ar for 30 min. Through a syringe, TMSA (1.5 mL, 10.6 mmol) was added and the mixture was stirred at room temperature in a sealed vessel overnight. The solvent was removed under reduced pressure and the crude mixture was run through a

silica plug (5:1 hexanes/CH_2Cl_2, 300 mL) and then concentrated. The residue was dissolved in DIPA (100 mL) and THF (100 mL), CuI (125 mg, 0.7 mmol), and $PdCl_2(PPh_3)_2$ (251 mg, 0.033 mmol) were added, then the mixture was degassed under Ar for 30 min. Through a syringe, TIPSA (10 mL, 47 mmol) was added and the mixture was stirred at room temperature in a sealed vessel overnight. The solvent was removed under reduced pressure and the residue was chromatographed on silica (hexanes) to afford **20** (3.2 g, 91%) as an orange oil. ^{1}H NMR (300 MHz, $CDCl_3$) δ 0.24 (s, 9H), 1.15 (s, 21H), 6.98 (d, J = 5.3 Hz, 1H), 7.08 (d, J = 5.3 Hz, 1H); ^{13}C NMR (75 MHz, $CDCl_3$) δ −0.1, 18.8, 98.0, 98.3, 98.7, 100.0, 125.5, 127.0, 127.2, 129.8; IR (NaCl) υ 2153, 2865, 2993, 2943 cm^{-1}; MS (APCI) m/z (%) 431.2 (100, M^+ + THF), 359.1 (30); HRMS (EI) for $C_{20}H_{23}SSi_2$ $[M]^+$ calcd 360.1770, found 360.1763.

3-(Triisopropylsilylethynyl)-4-(trimethylsilylethynyl)thiophene (22). 3-Bromo-4-iodothiophene (**17**, 4.7 g, 15.4 mmol), CuI (29 mg, 0.15 mmol), $PdCl_2(PPh_3)_2$ (61 mg, 0.075 mmol), and TMSA (2.40 mL, 17.0 mmol) were reacted as described above for **20**. The solvent was removed under reduced pressure and the crude mixture was run through a silica plug (hexanes) and then concentrated. The residue was dissolved in THF (20 mL) and DIPA (20 mL), CuI (29 mg, 0.15 mmol), and $Pd(PPh_3)Cl_2$ (41 mg, 0.05 mmol) were added, then the mixture was degassed under Ar for 30 min. $Pd(PPh_3)_4$ (26 mg, 0.025 mmol) and TIPSA (4.48 mL, 20.0 mmol) were added next. The reaction mixture was stirred in a sealed pressurized vessel at 115 °C for 4 d. Upon cooling, the solvent was removed in vacuo and the residue was chromatographed (hexanes) to afford **22** (4.2 g, 88%) as an orange oil. ^{1}H NMR (300 MHz, $CDCl_3$) δ 0.23 (s, 9H), 1.14 (s, 21H), 7.38−7.42 (m, 2H); ^{13}C NMR (75 MHz, $CDCl_3$) δ −0.1, 18.7, 92.8, 96.4, 98.1, 99.8, 125.0, 125.2, 129.0, 129.3; IR (NaCl) υ 2158, 2865, 2893, 2944, 3110 cm^{-1}; MS (APCI) m/z (%) 431.2 (40, M^+ + THF); HRMS (EI) for $C_{20}H_{23}SSi_2$ $[M]^+$ calcd 360.1763, found 360.1763.

General Procedure for Preparation of "Symmetrical" Annulene Precursors. To a solution of diyne (2.5 equiv) dissolved in MeOH/THF (10:1, 0.05 M) was added K_2CO_3 (10 equiv) and the mixture was stirred for 30 min. The solution was filtered and then Et_2O was added. The solution was washed successively with H_2O, 10% NaCl solution, and water, then dried ($MgSO_4$). Solvent was removed in vacuo and the residue was added to a solution of THF/DIPA (1:1, 0.1 M) and dihaloarene (1 equiv). The mixture was degassed under Ar for 30 min after which CuI (6 mol %) and $Pd(PPh_3)_4$ (3 mol %) were added. The sealed vessel was stirred at room temperature until TLC showed the reaction complete (12 h to 2 d). The solvent was removed in vacuo and the crude product was chromatographed on silica to afford the annulene precursor.

Tetrayne 25. Chromatography on silica (10:1 hexanes:CH_2Cl_2) furnished **25** (251 mg, 86%) as an orange oil. ^{1}H NMR (300 MHz, $CDCl_3$) δ 1.13 (s, 42H), 7.04 (d, J = 5.3 Hz, 2H), 7.17 (d, J = 5.3 Hz, 2H), 7.30 (*AA*′BB′m, 2H), 7.51 (AA′*BB*′m, 2H); ^{13}C NMR (75 MHz, $CDCl_3$) δ 11.3, 18.7, 86.3, 95.2, 95.8, 100.7, 125.4, 126.3, 126.90, 126.92, 128.1, 129.9, 131.5; IR (NaCl) υ 2149, 2213, 2863, 2941 cm^{-1}; MS (ACPI) m/z (%) 723.3 (20, M^+ + THF), 651.2 (100, MH^+); HRMS (EI) for $C_{40}H_{50}S_2Si_2$ $[M]^+$ calcd 650.2892, found 650.2901.

General Procedure for Preparation of "Asymmetrical" Annulene Precursors. To a solution of diyne (1.0 equiv) dissolved in MeOH/THF (10:1, 0.05 M) was added K_2CO_3 (2.5 equiv) and the mixture was stirred for 30 min. The solution was filtered and then Et_2O was added. The solution was washed successively with H_2O, 10% NaCl solution, and water, then dried ($MgSO_4$). Solvent was removed in vacuo and the residue was added to a solution of THF/DIPA (1:1, 0.1 M) and dihaloarene (1 equiv). The mixture was degassed under Ar for 30 min after which CuI (6 mol %) and $Pd(PPh_3)_4$ (3 mol %) were added. The sealed vessel was stirred at room temperature until TLC showed the reaction complete (12 h to 2 d). The solvent was removed in vacuo and the crude product was chromatographed on a short plug of silica to afford the halodiyne precursor. This material was redissolved in THF/DIPA (1:1, 0.1 M) and the second diyne (1.5 equiv), desilylated in the manner described above, was added. The solution was degassed under Ar for 30 min and then CuI (6 mol %) and $Pd(PPh_3)_4$ (3 mol %) were added. The sealed vessel was stirred at room temperature until TLC showed the reaction complete (12 h to 2 d). The solvent was removed in vacuo and the crude product was chromatographed on silica to afford the annulene precursor.

Tetrayne 26. Chromatography on silica (10:1 hexanes:CH_2Cl_2) furnished **27** (702 mg, 81%) as an orange oil. ^{1}H NMR (300 MHz, $CDCl_3$) δ 1.11 (s, 21H), 1.12 (s, 21H), 7.03 (d, J = 5.3 Hz, 1H), 7.04 (d, J = 5.3 Hz, 1H), 7.08 (d, J = 5.3 Hz, 1H), 7.14 (d, J = 5.3 Hz, 1H), 7.17 (d, J = 5.3 Hz, 1H), 7.28 (d, J = 5.3 Hz, 1H); ^{13}C NMR (75 MHz, $CDCl_3$) δ 11.3, 18.66, 18.73, 85.3, 85.8, 91.7, 92.4, 95.4, 98.0, 100.6, 100.9, 125.7, 126.2, 126.27, 126.30, 126.58, 126.60, 126.76, 126.82, 129.2, 129.6, 129.9, 130.1; IR (NaCl) υ 2146, 2192, 2864, 2890, 2942 cm^{-1}; MS (ACPI) m/z (%) 657.2 (100, MH^+), 729.3 (90, MH^+ + THF); HRMS (MALDI) $C_{38}H_{48}S_3Si_2$ $[M]^+$ calcd 656.2457, found 656.2455.

General Procedure for Annulene Formation. To a solution of annulene precursor (1 equiv) in THF (0.1 M) was added TBAF (20 equiv, 1.0 M THF). The mixture was stirred for 5 min and then Et_2O was added. The solution was washed 4−6 times with brine and then water, and the organic layer was dried ($MgSO_4$). The solution was concentrated, rediluted with 1:1 THF/DIPA to ca. 50 mL, and then injected over 8 h via syringe pump into a THF/DIPA solution (1:1, 0.05 M) containing $PdCl_2$(dppe) (3 mol %), CuI (6 mol %), and I_2 (0.5 equiv). Once TLC showed completion of the reaction, the solvent was removed under reduced pressure and the residue was run through a silica plug (1:1 hexanes:CH_2Cl_2). The product was further purified on a chromatotron (8:1 hexanes:EtOAc) to afford the annulene as an unstable tan solid, which should be stored cold, in the dark, and under an Ar atmosphere to minimize decomposition.

[14]DBTA 6. Yield 9.7 mg, 53%. ^{1}H NMR (300 MHz, C_6D_6) δ 6.50 (d, J = 5.3 Hz, 2H), 6.68 (d, J = 5.3 Hz, 2H), 6.95 (*AA*′BB′m, 2H), 7.71 (AA′*BB*′m, 2H); ^{13}C NMR (75 MHz, CD_2Cl_2) δ 81.9, 85.3, 87.5, 99.2, 122.3, 124.6, 126.4, 128.3, 128.6, 132.6, 135.4; IR (KBr) υ 2102, 2924, 3102 cm^{-1}; UV (CH_2Cl_2) λ_{max} (log ε) 309 (4.44), 316 (4.46), 329.0 (4.74), 363 (4.74), 373 (3.90) nm; MS (APCI) m/z (%) 409.0 (100, MH^+ + THF); HRMS (EI) $C_{22}H_8S_2$ $[M]^+$ calcd 336.0067, found 336.0067.

[14]DTA 12. Yield 34 mg, 64%. ^{1}H NMR (300 MHz, C_6D_6) δ 6.46 (d, J = 5.3 Hz, 1H), 6.53 (d, J = 5.3 Hz, 1H), 6.61 (d, J = 5.3 Hz, 1H), 6.77 (d, J = 5.3 Hz, 1H), 7.02 (d, J = 5.3 Hz, 1H), 7.18 (d, J = 5.3 Hz, 1H); ^{13}C NMR (75 MHz, C_6D_6) δ 82.9, 83.3, 86.5, 87.0, 87.9, 89.9, 95.0, 96.0, 123.2, 123.9, 124.3, 125.5, 126.4, 127.0, 127.3, 129.8, 132.2, 133.4; IR (KBr) υ 2140, 2183, 2871, 2959, 2982, 3109 cm^{-1}; UV (CH_2Cl_2) λ_{max} (log ε) 335 (4.99), 319 (4.74), 379 (4.28), 385 (4.26) nm; MS (APCI) m/z (%) 415.0 (100, MH^+ + THF); HRMS (MALDI) $C_{20}H_6S_3$ $[M]^+$ calcd 341.9632, found 341.9636.

Acknowledgement. We thank the ACS Petroleum Research Fund and the National Science Foundation (CHE-0718242) for financial support. We thank Prof. J. E. Hutchison for use of his group's potentiostat. We also thank the UO Neuroinformatics Center for use of the ICONIC Grid, a high-performance computational infrastructure constructed with support from NSF-MRI grant BCS-0321388.

Supporting Information Available: Experimental details for all new compounds; calculated HOMO/LUMO plots of **10**−**14**; CVs of selected annulenes; copies of ^{1}H and ^{13}C NMR spectra; computational details; CIF files for **8** and **13**. This material is available free of charge via the Internet at http://pubs.acs.org.

JO800225U